ARTICLE IN PRESS

Nano Communication Networks ▮ (▮▮▮▮) ▮▮▮–▮▮▮

Contents lists available at ScienceDirect

Nano Communication Networks

journal homepage: www.elsevier.com/locate/nanocomnet

Opto-ultrasonic communications for wireless intra-body nanonetworks

G. Enrico Santagati, Tommaso Melodia *

University at Buffalo, The State University of New York, Buffalo, NY, USA

ARTICLE INFO

Article history:
Received 31 October 2013
Received in revised form 2 March 2014
Accepted 3 March 2014
Available online xxxx

Keywords:
Opto-ultrasonic communications
Intra-body nanonetworks
Acoustic communications and networks

ABSTRACT

Wirelessly interconnected nanorobots, i.e., engineered devices of sizes ranging from one to a few hundred nanometers, are promising revolutionary diagnostic and therapeutic medical applications that could enhance the treatment of major diseases. Each nanorobot is usually designed to perform a set of basic tasks such as sensing and actuation. A dense wireless network of nano-devices, i.e., a nanonetwork, could potentially accomplish new and more complex functionalities, e.g., in-vivo monitoring or adaptive drug-delivery, thus enabling revolutionary nanomedicine applications.

Several innovative communication paradigms to enable nanonetworks have been proposed in the last few years, including electromagnetic communications in the terahertz band, or molecular and neural communications. In this paper, we propose and discuss an alternative approach based on establishing intra-body opto-ultrasonic communications among nanorobots. Opto-ultrasonic communications are based on the optoacoustic effect, which enables the generation of high-frequency acoustic waves by irradiating the medium with electromagnetic energy in the optical frequency range. We first discuss the fundamentals of nanoscale opto-ultrasonic communications in biological tissues by modeling the generation, propagation and detection of opto-ultrasonic waves, and we explore important tradeoffs. Then, we discuss potential research challenges for the design of opto-ultrasonic nanonetworks of implantable devices at the physical, medium access control, and network layers of the protocol stack.

© 2014 Elsevier Ltd. All rights reserved.

1. Introduction

Wirelessly interconnected nanorobots,[1] i.e., devices of sizes ranging from one to a few hundred nanometers, are a promising solution for remote and distributed medical diagnosis and treatment of major diseases [2]. Each nanorobot is usually designed to perform a set of basic tasks such as sensing and actuation. A dense wireless interconnection of nanodevices, i.e., a nanonetwork, could potentially accomplish new and more complex functionalities, e.g., in-vivo monitoring or adaptive drugs delivery, thus enabling revolutionary nano-medicine applications. Nano-sensors and nano-actuators distributed in the human body could enable pervasive and reactive continuous in-vivo monitoring. Pressure nano-sensors deployed in the eye can be helpful for high intraocular pressure (IOP) for early diagnosis and treatment of glaucoma to prevent vision loss, while monitoring bone-growth in young diabetes patients could help in preventing and treating osteoporosis. Wirelessly controlled nanorobots may be used to detect and eliminate malicious agents and cells inside biological tissues, e.g., viruses and cancer cells, enabling less invasive and less aggressive treatments [3,4]. Moreover, networked

* Corresponding author. Tel.: +1 716 645 1027.
E-mail addresses: santagat@buffalo.edu (G.E. Santagati), tmelodia@buffalo.edu (T. Melodia).

[1] A preliminary version of this paper [1] appeared in the Proceedings of the Asilomar Conference on Signals, Systems, and Computers, Asilomar, CA, 2013.

http://dx.doi.org/10.1016/j.nancom.2014.03.001
1878-7789/© 2014 Elsevier Ltd. All rights reserved.

nano-devices will be used for organ, nervous track, or tissue replacements, i.e., bio-hybrid implants.

Several innovative communication paradigms have been proposed during the last few years, including terahertz band communications [5,6], or molecular and neural communications [7–9]. In this paper, we take a different approach and investigate and study the use of ultrasonic waves to enable wireless networking between intra-body nanorobots.

Ultrasounds are mechanical waves that propagate in an elastic medium at frequencies above the upper limit for human hearing, i.e., 20 kHz. Acoustic waves are known to propagate better than their radio frequency (RF) counterpart in media composed mainly of water and have been used successfully for underwater communications [10,11]; and for ultrasonic imaging [12,13]. In [14–16], we showed that ultrasonic waves have a strong potential to enable internetworking among implanted devices in the human body at communication ranges spanning from few μm to several cm; while in [17] the authors, based on consideration on the physics of ultrasound propagation, investigate the power requirements for acoustic communications between nanorobots across various distances and tissues. However, as of today and to best of our knowledge, no existing studies have explored the feasibility of ultrasonic wave generation and detection at the nanoscale for communication purposes; moreover, no previous work has investigated communication and networking principles necessary to build the foundation of ultrasonic nanonetworks.

Ultrasounds are typically generated through *piezoelectric* materials that convert electrical energy into mechanical energy and vice versa [18]; or through the vibration of a thin plate, i.e., a capacitor, under *electrostatic* forces [19]. Microelectro-mechanical system (MEMS) technology enables the fabrication of both microscopic piezoelectric and electrostatic ultrasonic transducers, i.e., piezoelectric micromachined ultrasonic transducers (pMUTs) [20], and capacitive micromachined ultrasonic transducers (cMUTs) [21].

However, microscopic transducers do not satisfy the size requirements for being embedded into devices with nanoscopic dimensions, i.e., nanorobots. While, to best of our knowledge, no reports of nanoelectro-mechanical system (NEMS) ultrasonic transducers have appeared in the literature yet, initial successful attempts at developing nano-ultrasonic transducers based on the optoacoustic effect [22] have been reported.

The *optoacoustic* effect is a special case of a broader effect known as the *photoacoustic* effect. Photoacoustic effects in general refer to the generation of acoustic waves by any type of electromagnetic (EM) radiation, from radio frequency to X-ray. When the mechanical excitation is generated by a radio frequency wave, the phenomenon is referred to as *thermoacoustic* effect, while it is typically referred to as *optoacoustic* effect when the excitation frequency wave is in the optical range. In optoacoustics, acoustic waves can be generated through various mechanisms, including optical breakdown, vaporization, and thermoelastic generation [23]. In this paper, we consider the thermoelastic mechanism, where the energy irradiated by a laser is absorbed by the tissue surface or by an intermediate material causing rapid heating, and thus thermoelastic expansion, which in turn generates ultrasonic waves. Faster transient heating generates higher frequency components. For example, optical pulses a few nanoseconds long can generate ultrasonic pulses with central frequency and bandwidth in the order of hundreds of MHz [24]. We refer to ultrasonic waves generated through optical sources as opto-ultrasonic waves.

The photoacoustic effect was discovered in 1880 by A.G. Bell [25], who observed that a pulsed source irradiating a solid substrate can produce a sound wave. In the last decade, the photoacoustic effect has found extensive application in biomedicine and three-dimensional imaging, since it combines the high resolution of ultrasonic waves with the high contrast that characterizes light absorption. Indeed, optoacoustic imaging can be seen as an ultrasound-mediated EM imaging modality or an ultrasound imaging modality with EM-enhanced contrast [26].

The joint use of light beams and ultrasonic waves that characterizes optoacoustics could potentially be the foundation of a new communication paradigm to enable intra-body networking at the nanoscale. In fact, EM waves in the optical frequency range do not propagate easily in tissues; while ultrasonic waves propagate fairly well in media composed mainly of water. At the same time, generating and detecting ultrasounds through pulsed lasers has several advantage with respect to traditional ultrasonic transducers such as piezoelectric and capacitive transducers. In fact, optoacoustic sources and receivers offer very high miniaturization, high bandwidth and high sensitivity as compared to competing solutions [24,22]. Moreover, direct generation of ultrasonic waves in tissues may reduce energy losses associated with the coupling between the transducer surface and the tissue itself. Finally, recent advances in nano-optics have made the design and fabrication of nanoscopic optical sources, i.e., nanolasers, possible [27–29]. However, photoacoustic generation of ultrasounds also introduces significant challenges that need to be addressed to enable the design of transmission schemes and networking protocols for intra-body nanonetworks.

In this paper, we discuss the fundamentals of nanoscale opto-ultrasonic communications in biological tissues. We first model the generation, propagation and detection of opto-ultrasonic waves, and explore relevant design tradeoffs. Then, we discuss potential research challenges for the design of opto-ultrasonic nanonetworks of implantable devices at the physical (PHY), medium access control (MAC) and network layers of the protocol stack.

The rest of the paper is organized as follows. In Section 2, we discuss the potential hazards posed by using opto-ultrasonic communications in the human body. In Sections 3–5, we model the opto-ultrasonic wave generation, propagation, and detection, respectively. In Section 6 we discuss the design challenges of opto-ultrasonic communications in the human body at different levels of the protocol stack. Finally, in Section 7, we conclude the paper.

Please cite this article in press as: G.E. Santagati, T. Melodia, Opto-ultrasonic communications for wireless intra-body nanonetworks, Nano Communication Networks (2014), http://dx.doi.org/10.1016/j.nancom.2014.03.001

2. Opto-ultrasonic waves and health concerns

When generating opto-ultrasonic waves, the human body is exposed to both electromagnetic energy, in the optical frequency range, and to acoustic energy, in the ultrasonic frequency range. In this section, we discuss the potential hazards of using opto-ultrasonic communications in the human body, and we report reference values of maximum tolerable energy levels for both optical and acoustic radiations in biological tissues.

2.1. Optical bioeffects

Opto-ultrasonic waves are generated through various optoacoustic mechanisms, such as optical breakdown, vaporization and thermoelastic generation [23]. The efficiency of the generation mechanism is measured in terms of the *optoacoustic generation efficiency* η, that is, the ratio between the acoustic energy generated over the optical energy absorbed. Optical breakdown is the most efficient mechanism, and it occurs when high levels of optical energy ionize a tissue, thus forming a plasma that generates a pressure wave while expanding. Optical breakdown is characterized by a high generation efficiency, e.g., up to 30% in liquid, but requires extremely high laser intensities, above 10^{11} W/cm^2 [30,31]. When the optical energy absorbed by the tissue is lower than the breakdown threshold, but exceeds the boiling threshold, e.g., 2600 J/cm^3 for water, vaporization occurs, producing an opto-ultrasonic wave with efficiencies from 0.01% to 1% [32]. Finally, laser intensities lower than the breakdown and vaporization thresholds produce the so-called thermoelastic mechanism, where the absorbed energy generates a temperature gradient that leads to a thermal expansion, and therefore to the generation of opto-ultrasonic waves. This mechanism presents relatively low generation efficiency, in the range of 10^{-6}–10^{-5} [32,33], but it is in general more attractive because of its non-destructive and low-thermal effect properties. The thermoelastic effect can be further classified in two distinct modes, a *continuous-wave* mode and *pulse-based* mode [34]. The former consists of exciting the tissue with a pulsed light beam with a 50% duty cycle, while the latter is based on a very low duty cycle but higher intensity peaks. Pulse-based generation creates high-frequency ultrasonic waves with higher optoacoustic conversion efficiency, while the low duty cycle can further reduce the potential overheating caused by consecutive laser excitations. Since nanorobot communications need to be non-destructive, we focus on thermoelastic generation only, in particular in the *pulse-based mode*. Thus, in the rest of this paper, we assume that optical excitation energies are lower than the breakdown and vaporization thresholds. Moreover, we assume that the excitation energy is lower than a safety threshold given by the maximum permissible exposure (MPE) recommendations defined by the American National Standards Institute (ANSI) [35]. For example, in terms of irradiance, i.e., the laser intensity expressed in W/cm^2, ANSI recommend a 10^{-3} W/cm^2 limit for optical radiation in the 400–700 nm wavelength range, i.e., visible range, and $10^{2(\lambda-0.7)}$ in the 700–1050 nm wavelength range, i.e., part of the near infrared range, with λ being the wavelength of the optical radiation in microns. The ANSI standard also defines formulas to determine the *repetitive excitation* MPE for different wavelength ranges, pulse repetition frequencies, and single-pulse durations.

2.2. Acoustic bioeffects

The most well-understood acoustic effect in biological tissues is *heating*. During ultrasound propagation, a portion of the energy is absorbed and converted into heat, which could lead to a temperature increase. A linear relationship between ultrasound intensity (i.e., power carried by the wave per unit of surface) and temperature rise has been demonstrated [36,37]. It was also shown that the relative protein content of tissues and the propagating frequency contribute to determining ultrasound absorption, which can vary from 0.212 Np cm^{-1} MHz^{-1} in skin up to 1.8 Np cm^{-1} MHz^{-1} in bones [38]. Also, exposure time plays an important role in the heating effect. An increase in temperature occurs if heat generation due to ultrasound absorption is greater than heat dissipation through blood circulation in the tissue, i.e., tissue perfusion. As the wave intensity increases, the temperature rises and if it becomes higher than 38.5 °C, adverse biological effects may occur. Since heating is caused by the intensity of the wave, impulsive transmissions with a low duty cycle can potentially reduce this effect by a factor proportional to the duration of the duty cycle.

Another effect caused by ultrasonic wave propagation is *cavitation*, which denotes the behavior of gas bubbles within an acoustic field. Pressure variations of the ultrasound wave cause bubbles in the propagation medium to contract and expand. For large pressure variations, the bubble size drastically increases, reaching an expansion peak when pressure is minimum and then collapsing when pressure reaches its peak. During this process, the internal pressure and temperature in the bubble can reach high values causing serious biological effects and damaging tissues located in close proximity. Cavitation is a frequency-dependent phenomenon. Since at higher frequencies there are shorter pressure oscillations, the bubble expansion time is reduced and the cavitation effect tends to disappear. Impulsive transmissions may also contribute to reducing cavitation effects, since during the off period bubbles tend to return to their original size without imploding. Destructive cavitation effects have not been reported at intensity values less then 10^4 pW/μm^2 [39,17].

Mechanical effects of ultrasounds in tissues also include structural and functional injuries that can affect biological cells when exposed to pressure waves. This effects are proportional to the pressure peak and repetition of the stress applied, but also depend on the cell type and the activity of the cells [40]. Experimental results report damage thresholds in the order of 10^6 Pa [40,17].

Ultrasounds have been successfully used for therapeutic and diagnostic purposes inside the human body since the 1960s with no detrimental effects. The medical experience of the last decades has demonstrated that ultrasound is fundamentally *safe*, as long as tissues are exposed to acoustic intensities below 10^3 pW/μm^2 for

Please cite this article in press as: G.E. Santagati, T. Melodia, Opto-ultrasonic communications for wireless intra-body nanonetworks, Nano Communication Networks (2014), http://dx.doi.org/10.1016/j.nancom.2014.03.001

unfocused ultrasounds [41]. A safe value of 10^4 pW/μm^2 is also considered for ultrasounds produced by a focused transducers whose focal length[2] is regulated through a lens to a desired value [41]. The resulting pressure peak limits, assuming a micron-sized acoustic source, and considering the quadratic relationship between acoustic intensity and pressure $I = \frac{P_{\text{peak}}}{2\rho c}$, with ρ and c the density and speed of sound in the tissue [14], are approximately $0.06 \cdot 10^6$ and $0.17 \cdot 10^6$ Pa for unfocused and focused ultrasound, respectively. These pressure values are one or two orders of magnitude lower than the cell damage thresholds discussed above. In general, such detrimental effects have not been observed when the acoustic energy imparted to the tissue, i.e., the product of intensity and exposure time, is less than 50 J/cm^2 [41,14]. Therefore, ultrasounds at low transmission pressure levels, and consequently low transmission power levels, are known to not cause any lethal bioeffects. Thus, opto-ultrasonic communications can be a safe and reliable alternative to classical electromagnetic RF communications.

3. Opto-ultrasonic wave generation

In this section, we model the generation of opto-ultrasonic waves and characterize the generated signal both in the time and frequency domain. We show how the temporal profile of the signal, and hence its frequency spectrum, depend on (i) the duration of the optical excitation and (ii) the width of the optical beam. Moreover, we observe that the amplitude of the generated signal depends on the intensity of the optical excitation and the characteristics of the radiated tissue. We also discuss the issue of optical source selection, and present potential techniques that can be adopted to increase the conversion efficiency of thermoelastic ultrasound generation.

3.1. Thermoelastic generation model

As discussed in Section 2, when the intensity of the laser exciting the tissue is lower than the breakdown and vaporization thresholds, opto-ultrasonic wave generation is based on the thermoelastic mechanism.

Assume a stationary and non-viscous soft-tissue with negligible thermal conductivity. Under these conditions, if sound speed and density are constant in space, the acoustic pressure as a function of time t and space vector $\mathbf{r}$, $P(\mathbf{r}, t)$, in the linear acoustic approximation and in the absence of absorption, obeys the acoustic wave equation [42],

$$\frac{\partial^2 P(\mathbf{r}, t)}{\partial t^2} - c^2 \nabla^2 P(\mathbf{r}, t) = \Gamma \frac{\partial \mathcal{H}(\mathbf{r}, t)}{\partial t}, \tag{1}$$

where c (m/s) is the speed of sound, $\Gamma = \frac{\beta c^2}{C_p}$ is the dimensionless Grüneisen coefficient, which measures the conversion efficiency from optical energy to pressure, β (K^{-1}) is the thermal volume expansion coefficient, C_p (J Kg^{-1}K^{-1}) is the specific heat capacity of the medium, and $\mathcal{H}(\mathbf{r}, t)$ (J m^{-3}s^{-1}) is the heat energy absorbed by the tissue per unit time and unit volume. If we assume the source to be stationary, the heating component can be written as $\mathcal{H}(\mathbf{r}, t) = E_a G(\mathbf{r}) T(t)$, where $T(t)$ (s^{-1}) and $G(\mathbf{r})$ (m^{-3}) represent the temporal profile and the radial profile of the heat source, respectively, and are related to the radiating source, i.e., the beam diameter and the duration of the pulses. The term E_a (J) is the total energy absorbed by the tissue. The total energy absorbed can be further expressed as $E_a = \mu_a F$, where μ_a is the absorption coefficient (m^{-1}) and F is the beam *local fluence* (J m^{-2}). Under very-short optical pulse excitation, the absorbed heat becomes $\mathcal{H}(\mathbf{r}, t) = E_a G(\mathbf{r}) \delta(t)$, where $\delta(t)$ is the *Dirac* function. Under this condition, the wave equation becomes:

$$\frac{\partial^2 P(\mathbf{r}, t)}{\partial t^2} - c^2 \nabla^2 P(\mathbf{r}, t) = 0, \tag{2}$$

with initial values $P(\mathbf{r}, 0) = \Gamma E_a G(\mathbf{r})$ and $\frac{\partial P(\mathbf{r},0)}{\partial t} = 0$. Thus the initial pressure, $P(\mathbf{r}, 0)$ is directly proportional to the absorbed energy density $E_a G(\mathbf{r})$.

The above equation gives us a solution for an ideal instantaneous radiation. The solution for a finite, hence real, pulse can be found by calculating the convolution between the ideal solution and the temporal laser pulse profile [43]. Specifically, let us assume a spherical Gaussian radial and temporal profile for the source

$$G(r) = \frac{1}{(2\pi)^{3/2} R^3} e^{-\frac{1}{2}\left(\frac{r}{R}\right)^2}, \tag{3}$$

$$T(t) = \frac{1}{\sqrt{2\pi\,\tau_l^2}} e^{-\frac{1}{2}\left(\frac{t}{\tau_l}\right)^2}, \tag{4}$$

where R is the radius of the sphere, and τ_l is the characteristic width of the temporal profile.[3] Under this assumption, the radial profile $G(\mathbf{r})$ depends only on the radial component of the vector $\mathbf{r}$, i.e., the Euclidean norm, which we denote as r. Under far-field condition ($r \gg R$), we obtain the following pressure field generated [44]

$$P(r, t) = -\frac{\beta E_a}{2(2\pi)^{3/2} C_p r} \frac{t - \tau}{\tau_e^3} e^{-\frac{1}{2}\left(\frac{t-\tau}{\tau_e}\right)^2}, \tag{5}$$

where $\tau = \frac{r}{c}$, $\tau_a = \frac{R}{c}$ and $\tau_e = \sqrt{\tau_a^2 + \tau_l^2}$. According to this model, τ_e, i.e., the effective characteristic width of the optoacoustic temporal profile, depends on both *the duration* of the optical pulse and on *the width* of the optical beam. As a consequence, sources with different radial profiles generate optoacoustic waves of different frequency for the same incident light pulse. For example, a larger diameter beam produces a lower frequency wave for the same temporal profile with respect to a smaller diameter beam. The opposite is also true. We also observe that the amplitude of the generated pulse depends linearly on the thermal expansion coefficient β and on the energy absorbed E_a, i.e., from

[2] The distance from the transducer to the point of maximum signal amplitude.

[3] Half the pulse duration between the $1/e$-points of the temporal amplitude distribution.

Please cite this article in press as: G.E. Santagati, T. Melodia, Opto-ultrasonic communications for wireless intra-body nanonetworks, Nano Communication Networks (2014), http://dx.doi.org/10.1016/j.nancom.2014.03.001

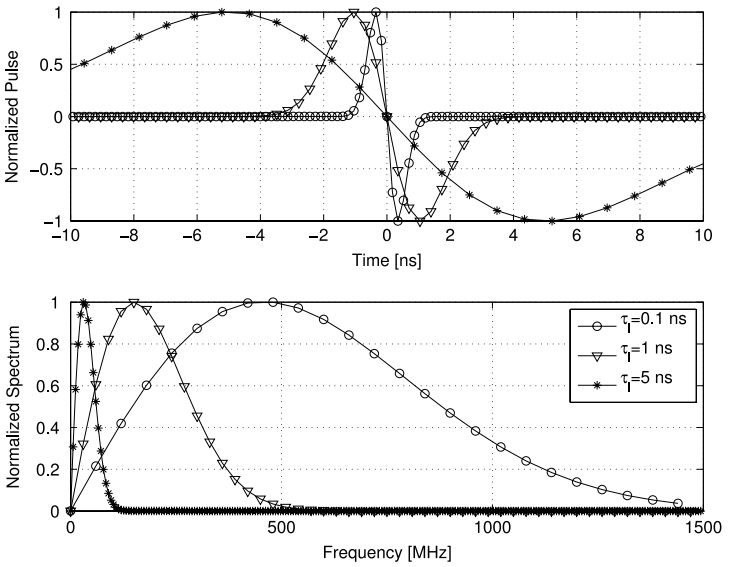

Fig. 1. Normalized temporal profile and normalized spectrum of the generated opto-ultrasonic pulse for different characteristic widths of the temporal profile τ_l and with sphere radius $R = 500$ nm.

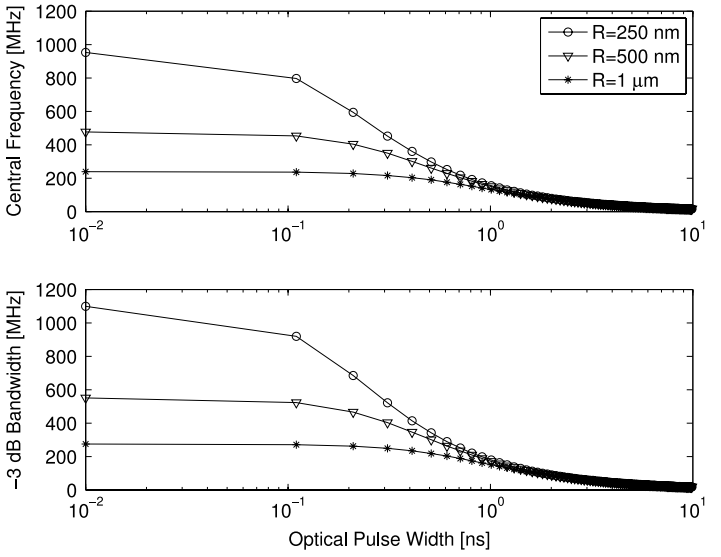

Fig. 2. Central frequency and −3 dB bandwidth of the generated opto-acoustic signal as a function of τ_l for three different values of the sphere radius R.

the absorption coefficient μ_a of the tissue at that specific optical wavelength and the radiated laser energy F.

Based on these observations, to operate at desired frequency and acoustic intensity ranges, i.e., spectrum central frequency, bandwidth, and signal amplitude, the optical excitation source must be tuned accordingly.

Opto-ultrasonic frequency spectrum. We now quantitatively show how the opto-ultrasonic signal frequency spectrum depends on the optical pulse duration and the optical beam width. By Fourier-transforming (5), we obtain the amplitude spectrum of the generated signal [44]

$$|P(r,f)| = \frac{\beta E_a}{2C_p r} f e^{-2(\pi\tau_e f)^2}. \quad (6)$$

Figure 1 shows the normalized temporal profile and the normalized spectrum of the generated opto-ultrasonic pulse when varying the optical pulse duration, i.e., for different characteristic widths of the temporal profile τ_l. It is assumed that the radiating surface of the nanolaser is spherical with radius R of 500 nm. The generated optical beam is therefore also characterized by a radius R. We observe that shorter optical pulses have higher central frequency and a larger bandwidth. For example, with a 5 ns-long optical pulse, we obtain an opto-ultrasonic signal with central frequency of 150 MHz and about 170 MHz of −3 dB bandwidth. In Fig. 2, the central frequency and the −3 dB bandwidth of the generated opto-acoustic signal is plotted as a function of τ_l, for three different values of

Please cite this article in press as: G.E. Santagati, T. Melodia, Opto-ultrasonic communications for wireless intra-body nanonetworks, Nano Communication Networks (2014), http://dx.doi.org/10.1016/j.nancom.2014.03.001

the sphere radius R. We observe that, according to the sphere radius, when $\tau_l < \tau_a$, both the central frequency and the −3 dB bandwidth are strongly dependent on the sphere radius, but less dependent on the optical pulse duration. Instead, when the pulse duration becomes such that $\tau_l > \tau_a$, the opto-ultrasonic signal spectrum becomes independent of the beam radius and it only depends on the optical pulse duration. Therefore, for a given beam radius R, which depends on the nanorobot dimensions and the size of the optical source, there is a maximum frequency limit that cannot be overcome even by further reducing the optical pulse duration. For example, for a 500 nm-radius optical beam, the maximum achievable central frequency is about 500 MHz.

Based on the discussion above, we can conclude that the selection of the operating frequency is constrained by both the dimension of the optical source, i.e., the optical beam width, and the duration of the excitation pulse. Therefore, if we fix the size of the nanorobot, hence the size of the optical source, the opto-acoustic transmitter can tune the operating frequency by varying the duration of the optical excitation, up to the maximum frequency limit determined by the optical beam width.

3.2. Optical sources

The optical beam generated by a laser provides the medium with the energy, hence, the heat, required to trigger the thermoelastic effect that generates the opto-acoustic wave. Therefore, selecting the right optical source is crucial while designing an opto-ultrasonic communication system. Current optoacoustic applications, e.g., photoacoustic tomography (PAT), make use of externally located macroscopic lasers that irradiate the target tissue that needs to be scanned. Pulse lasers are commonly used, e.g., q-switched or mode-locked, that operate at optical wavelengths in the visible range 400–700 nm or in the near-infrared range 700–1400 nm [26]. The laser wavelength is selected to maximize the energy absorbed by the target tissue, and therefore, to increase the opto-ultrasonic generation efficiency.

To make opto-ultrasonic nanocommunications feasible, optical source dimensions need to be scaled in such a way as to meet the nanoscopic integration requirements. The miniaturization of lasers has been limited by the fact that the size of the optical resonator has to be greater than approximately half the optical beam wavelength in the laser medium, i.e., the diffraction limit. However, recent advances in nano-optics have made the design and fabrication of optical devices with subwavelength dimensions possible [27–29].

3.3. Optoacoustic amplification

The thermoelastic generation mechanism is in general characterized by relatively low generation efficiency. However, the thermoelastic efficiency can be improved by using materials with high thermal expansion coefficients and high optical absorption that can be interposed between the light source and the tissue, thus enhancing the efficiency of optoacoustic conversion. We refer to generation through intermediate materials as *indirect* optoacoustic generation, as opposed to the *direct* generation in tissues. The higher efficiency of indirect generation can be leveraged to produce higher-intensity opto-ultrasonic pulses, and therefore consider the intermediate material as an amplification stage in opto-ultrasonic transmitters.

A potential solution to amplify the signal consists of using a thin film metal or polymer-based absorber as intermediate material [45]. When irradiated by a laser, the thin film absorbs heat, and therefore it expands and radiates an acoustic wave into the surrounding medium. Because of the high optical absorption, the thin film generates higher-intensity opto-ultrasonic waves compared to direct generation. When thin films are used, the optical absorption is determined by the composition of the intermediate material. As a consequence, the opto-ultrasonic efficiency is virtually independent of the composition of the surrounding medium, and therefore independent of the location of the opto-ultrasonic source in the body. As an alternative, nanoscopic metal structures, e.g., gold nanoparticles, can be used as photoabsorbers. Nanoparticles exhibit special resonance effects at specific excitation wavelengths, which enable strong light absorptions [46]. By absorbing optical energy, nanoparticles generate heat that is transferred to the surrounding medium, which will then produce the opto-ultrasonic wave due to the thermoelastic effect. As for direct generation, the surrounding medium generates the opto-ultrasonic wave, while the nanoparticles behave as local heat sources. Because of the higher heat produced, the thermoelastic response of the tissue is greater than normal direct generation, which does not involve external photoabsorbers. Moreover, generation in the tissue avoids energy coupling problems that may occur with the thin-film-mediated generation.

4. Opto-ultrasonic wave propagation in tissues

In this section, we discuss some fundamental aspects of opto-ultrasonic propagation in tissues at the nanoscale level. First, we discuss opto-ultrasonic signal propagation in tissues in terms of attenuation, propagation delay and multipath effect. Based on this, we discuss criteria for selection of the optimal operating frequency.

4.1. Propagation effects

Attenuation. Two main mechanisms contribute to ultrasound attenuation in tissues, i.e., absorption and scattering. An initial pressure P_0 decays at a distance r according to [47]

$$P(r) = P_0 e^{-\alpha r}, \tag{7}$$

where α (in (Np cm^{-1})) is an amplitude attenuation coefficient that captures all the effects that cause dissipation of energy from the ultrasonic wave. Parameter α depends on the carrier frequency through $\alpha = af^b$, where f represents the carrier frequency (in MHz) and a (in (Np cm^{-1} MHz^{-b})) and b are attenuation parameters characterizing the tissue [14]. In biological tissues, and for frequencies in the range of few MHz, b is approximately equal to 1. When the

Please cite this article in press as: G.E. Santagati, T. Melodia, Opto-ultrasonic communications for wireless intra-body nanonetworks, Nano Communication Networks (2014), http://dx.doi.org/10.1016/j.nancom.2014.03.001

frequency range is higher than 10 MHz, b has values close to 2, as in pure water. Therefore, the attenuation coefficient increases quadratically with frequency [17].

By multiplying (6) by the frequency-dependent sound absorption in (7), we obtain

$$|P(r,f)| = \frac{\beta E_a}{2C_p r} f e^{-[2(\pi\tau_e f)^2 + raf^b]}. \quad (8)$$

If we assume to operate at frequencies greater than 10 MHz, hence $b = 2$, we can Fourier-invert (8) and obtain the opto-ultrasonic pressure field $P(r, t)$ in the presence of absorption. As a result, $P(r, t)$ is still described by (5), with the exception that the effective time constant is now

$$\tau_e'(r) = \sqrt{\tau_a^2 + \tau_l^2 + \frac{ra}{2\pi^2}}. \quad (9)$$

However, for short-range communication, i.e., $ra < \tau_e$, the absorption effect, therefore the exponential attenuation in (7), is relatively small when compared with the pressure decrease caused by spreading of the acoustic wave. Under these conditions, the initial pressure P_0 decreases in an inversely proportional way with respect to the distance r from the source [44].

Propagation delay. The propagation speed of acoustic waves in biological tissues is approximately 1500 m/s, with a small variation of less than 10% in most soft tissues, as compared to 2×10^8 m/s [48] for RF waves. However, for the relatively short communication ranges considered, i.e., in the order of a few hundreds of μm, the propagation delay is in the order of tens of nanoseconds. Moreover, since the internal body temperature is subject to small variations, i.e., a few °C, the temperature dependence of the speed of sound can be usually neglected for ultrasonic propagation in biological tissues.

Reflections and scattering. The human body is composed of different organs and tissues with different sizes, densities and sound speeds. Therefore, it can be modeled as an environment with pervasive presence of *reflectors* and *scatterers*. The direction and magnitude of the reflected wave depend on the orientation of the boundary surface and on the acoustic impedance of the tissues, Z measured in Rayl (kg s^{-1} m^{-2}) [14]. Scattered reflections occur when an acoustic wave encounters an object that is relatively small with respect to its wavelength or a tissue with an irregular surface. Consequently, the received signal is obtained as the sum of numerous attenuated, possibly distorted, and delayed versions of the transmitted signal.

In a nanoscopic scenario, the ultrasonic wavelength in biological tissues is of the order of a few μm at a frequency of a few hundreds of MHz. Therefore, it is equal to or larger than the size of any potential scatterer in the tissue, e.g., cell nuclei and organelles. As a consequence, the signal may be strongly affected by multipath due to scattering effect. Biological cells can potentially behave as scatterers according to their nucleus-to-cell-volume ratio, i.e., the ratio between the nucleus cell volume and the total cell volume. For example, cells with low nucleus-to-cell-volume ratio behave as a simple fluid cytoplasm sphere, thus producing limited scattering effect. Conversely, when the nucleus-to-cell-volume ratio is high, the scattering effect of the nucleus becomes significant, and it cannot be neglected anymore. Furthermore, intracellular organelles and protein molecules, although several orders of magnitude smaller than the ultrasonic wavelength, can behave as Rayleigh scatterers, thus affecting the signal propagation.

4.2. Operating frequency

Several key aspects need to be considered to determine an optimal operating frequency for intra-body opto-ultrasonic communications. Specifically, (i) the *attenuation coefficient* increases with frequency, quadratically when the frequency exceeds 10 MHz; (ii) the *beam spread* of the generated ultrasonic waves is inversely proportional to the ratio of the diameter of the radiating element and the wavelength [14]; (iii) the *ultrasonic power efficiency*, defined as the fraction of excitation power that produces acoustic radiation (and is not dissipated against viscous forces), increases with frequency [17]; finally, (iv) the *maximum achievable frequency* of the optoacoustic source is limited by its size, as discussed in Section 3. Therefore, one needs to operate at frequencies corresponding to the desired compromise between beam directivity and ultrasonic power efficiency, and that are at the same time compatible with the source dimension and the maximum tolerable attenuation.

In [14], we observed that, given the limited attenuation effect due to absorption in short-range communications, the operating frequency may be as high as 1 GHz. In [17], the authors observed that for a 500 nm-radius nanorobot the transmission efficiency, i.e., the fraction of emitted power that reaches a distance of 100 μm, which depends on both the attenuation and the ultrasonic power efficiency, has a maximum around 150 MHz. Finally, as reported in Section 3, the maximum achievable central frequency for a 500 nm-radium opto-ultrasonic source is approximately 500 MHz. Therefore, in accordance with our previous results in [14], we expect that opto-ultrasonic nanorobots communicating over short-range distances, i.e., less than a mm, will be able to optimally operate, with respect to maximum tolerated attenuation, transmission directivity, and transmission efficiency, at frequencies in the order of a few hundreds of MHz.

5. Opto-ultrasonic wave detection

In this section, we discuss optical detection of ultrasonic waves. This primarily consists of using light beams for detecting acoustic fields propagating in tissues. Specifically, we model an opto-ultrasonic detector based on an optical resonator, and we characterize this in terms of detection sensitivity and bandwidth. Results show that, differently from piezoelectric transducers, the receiver sensitivity is independent of the size of the active area of the detector. Moreover, the sensitivity and bandwidth mainly depend on the design of the optical resonator, i.e., the optical cavity length and the reflectivity of the resonator mirrors.

Please cite this article in press as: G.E. Santagati, T. Melodia, Opto-ultrasonic communications for wireless intra-body nanonetworks, Nano Communication Networks (2014), http://dx.doi.org/10.1016/j.nancom.2014.03.001

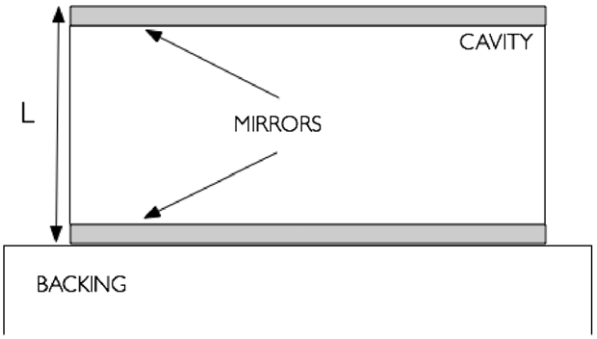

Fig. 3. Structure of an optical resonator.

5.1. Optical-ultrasonic detector

Optical detection of ultrasounds is based on measuring the variations induced by the acoustic field on a target optical field. Specifically, a laser source interrogates a reflecting surface coupled with the acoustic medium, and when the ultrasonic waves cause a displacement in the surface, this is translated in a phase shift of the laser beam. In other words, the acoustic wave reaching the surface phase-modulates the optical beam proportionally to the surface displacement. The modulated signal is then reflected, thus carrying back to the source the acoustic displacement information that can then be demodulated.

A similar and more efficient solution can be obtained by using an optical resonator as an ultrasound transducers, [22,49]. An optical resonator consists of an arrangement of mirrors that creates a standing wave cavity resonator for light waves [50], as in Fig. 3. With optical resonators, the interaction between the optical and acoustic fields takes place in a resonant cavity, and as a result, the laser beam is amplitude-modulated. In fact, the incident beam goes through several reflections in the resonant cavity, producing every time a reflected signal, i.e., the signal emitted in the direction opposite to the incident beam direction, whose intensity depends on the optical path length within the resonator. The displacement produced by the incident acoustic wave changes the cavity length, and hence modulates the intensity of the reflected signal. The design of opto-ultrasonic transceivers based on optical resonator principles has been proposed in [49], which includes both optoacoustic transmitter and detector. Moreover, plasmonic nanocavities that leverage surface plasmons to scale photonic devices beyond the diffraction limit of light have been thoroughly studied [51].

An optical resonator can be modeled as a Fabry–Pérot interferometer, also known as an *etalon* [52]. Given an incident light intensity I_0 (W m^{-2}), the reflected beam intensity is the complementary of the transmitted beam intensity, i.e., $I_R + I_T = I_0$, and can be expressed as

$$I_R = I_0 \left(1 - \frac{1}{1 + K \sin^2(\Phi/2)}\right), \tag{10}$$

where Φ (rad) is the round trip phase shift and is expressed as $\Phi = \frac{4\pi nL\nu}{c}$, where L (m) is the length of the resonator cavity, n is the index of refraction of the etalon material, c (m/s) is the speed of light, and ν (Hz) is the optical frequency. The coefficient K is given by $K = \frac{4R}{(1-R)^2}$, where R is the reflectivity of the resonator mirrors.

Receiver sensitivity. Using a first order approximation, for a small change in length δL, i.e., a small level of ultrasonic pressure reaching the receiver surface, the reflected light intensity variation is given by [49]

$$\delta I_R = \frac{\partial I_R}{\partial L}\delta L = \frac{4\pi nK \sin(\phi/2)\cos(\phi/2)}{\lambda(1 + K \sin^2(\phi/2))^2}\delta L. \tag{11}$$

Assuming near-resonance conditions, and calculating the phase shift that maximizes the reflected intensity in (11), i.e., the phase shift that results in maximum slope for the optical resonance [49], we obtain:

$$\delta I_R = I_0 \frac{9\pi}{4}\sqrt{\frac{K}{3}}\left(\frac{n\delta L}{\lambda}\right). \tag{12}$$

By defining the cavity finesse, $\mathcal{F}$ as

$$\mathcal{F} = \frac{\pi}{2}\sqrt{K}, \tag{13}$$

(12) can be rewritten as

$$\delta I_R = I_0 \frac{9}{2\sqrt{3}}\left(\frac{\mathcal{F} n\delta L}{\lambda}\right). \tag{14}$$

We observe that higher finesse results in higher ultrasonic detection sensitivity.

The receiver acoustic sensitivity S_r, i.e., the minimum pressure detectable by the receiver, can be obtained by considering the detectable displacement δL that produces a unitary signal-to-noise ratio, i.e., the minimum detectable displacement $\delta L_{\min}$ [49]. Assuming that the optical shot noise of the photodetector is the only noise source affecting the detection functionalities, the expression for the detection SNR can be written as

$$SNR = \frac{I_{SIG}^2}{I_{NOISE}^2} = \frac{SI_R^2}{2qBI_0}, \tag{15}$$

where S (A/W) is the optical detector sensitivity, q (C) is the electron charge, and B (Hz) is the detection bandwidth of the photodetector. For a small change in length δL, i.e., a low level of ultrasonic pressure reaching the receiver surface, we can substitute the first order approximation in (14) into (15), and obtain

$$SNR = \frac{27SI_0}{4qB}\left(\frac{\mathcal{F} n\delta L}{\lambda}\right)^2. \tag{16}$$

Please cite this article in press as: G.E. Santagati, T. Melodia, Opto-ultrasonic communications for wireless intra-body nanonetworks, Nano Communication Networks (2014), http://dx.doi.org/10.1016/j.nancom.2014.03.001

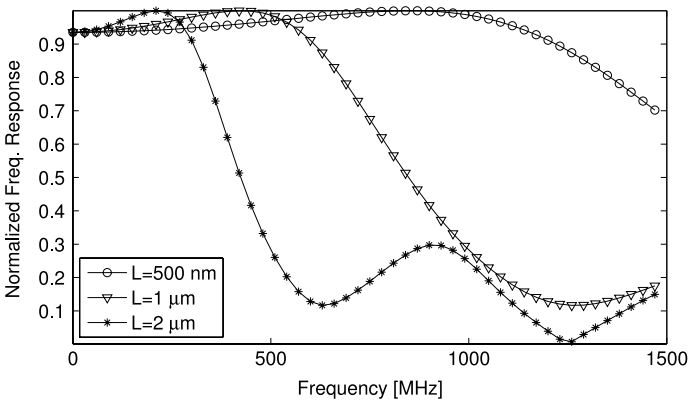

Fig. 4. Normalized frequency response of an etalon-based opto-ultrasonic detector.

From (16), the minimum detectable displacement $\delta L_{\min}$ can be obtained by setting the SNR equal to 1 as

$$\delta L_{\min} = \sqrt{\frac{4qB}{27SI_0}} \left(\frac{\lambda}{\mathcal{F}n}\right). \tag{17}$$

Finally, by considering the Young's modulus of the etalon Y (Pa), which establishes the relationship between the etalon deformation and the corresponding pressure, we can express the receiver acoustic sensitivity as

$$S_r = Y\frac{\delta L}{L} = \sqrt{\frac{4qB}{27SI_0}} \left(\frac{\lambda}{\mathcal{F}n}\right)\frac{Y}{L}. \tag{18}$$

We observe that the sensitivity of the receiver increases with higher finesse or with longer cavity. Moreover, from (13), we observe that the finesse depends only on the mirror reflectivity, and not on the cavity length. Therefore, the receiver sensitivity can be adjusted by independently tuning either the finesse or the cavity length. However, the cavity length is limited by the nanorobot dimensions. Another advantage is that the sensitivity does not depend on the dimension of the active area, defined by the diameter of the probing optical beam. Therefore, very small aperture and wideband ultrasound receivers still have high sensitivity, thus overcoming the limitations of piezoelectric transducers, whose sensitivity decreases with the element size [53].

Receiver bandwidth. The receiver bandwidth is determined by the frequency response of the optical cavity, which is obtained by considering the mean distribution of stress across the length of the resonator cavity caused by an incident acoustic wave [54,55],

$$|C(f)| \propto \frac{1}{f}\frac{\left|\left[e^{i\frac{2\pi f}{c}L}-1\right]+R_{a,1}\left[1-e^{-i\frac{2\pi f}{c}L}\right]\right|}{\left|1-R_{a,1}R_{a,2}e^{-i\frac{2\pi f}{c}2L}\right|}, \tag{19}$$

where L (m) is the length of the resonator cavity, and c is the speed of sound in the etalon material. $R_{a,1}$ and $R_{a,2}$ represent the acoustic reflection coefficient due to the acoustic impedance mismatch between the external medium, e.g., a biological tissue and the etalon material, and between the etalon material and the backing material, respectively. The acoustic reflection coefficient depends on the acoustic impedances of the two materials in the interface, Z_1 and Z_2, as $R_a = \frac{Z_1-Z_2}{Z_1+Z_2}$. Figure 4 shows the normalized frequency response of the etalon-based opto-ultrasonic detector for three different cavity lengths, assuming the external tissue to be skeletal muscle ($Z_{muscle} = 1.65$ MRayl) [14], the backing material to be glass ($Z_{glass} = 14.7$ MRayl), and the cavity material to be SU-8 photoresist ($Z_{SU-8} = 2.9$ MRayl), a polymer commonly used in the microelectronics industry [54]. The speed of sound c in the SU-8 is 2500 m/s. We observe that, by reducing the cavity length, the frequency response of the opto-ultrasonic detector shifts towards higher frequencies, thus offering significantly larger bandwidth. For example, by reducing the cavity length of the detector from 2 μm to 500 nm, the −3 dB bandwidth increases from approximately 400 MHz to more than 1 GHz.

Based on this, we observe that both detector sensitivity and detection bandwidth depend on the cavity length. The sensitivity increases by increasing the cavity length. On the contrary, the bandwidth increases by decreasing the cavity length. As a result, one cannot change the detection bandwidth without affecting the detector sensitivity. However, since the detector sensitivity also depends on the cavity finesse, that does not depend on the cavity length, one can tune the finesse and the length cavity independently to achieve the desired detection bandwidth and detector sensitivity.

6. Research challenges

In this section, we discuss future research challenges for the design of opto-ultrasonic intra-body nanonetworks at the physical (PHY), medium access control (MAC) and network layers of the protocol stack.

6.1. Physical layer

Ad-hoc physical layer solutions have be designed to optimally address the specific challenges posed by the use of opto-ultrasonic waves to interconnect nanorobots implanted in the human body:

Multipath effect. As discussed in Section 4, due to the inhomogeneities of the human body, the signal propagating

Please cite this article in press as: G.E. Santagati, T. Melodia, Opto-ultrasonic communications for wireless intra-body nanonetworks, Nano Communication Networks (2014), http://dx.doi.org/10.1016/j.nancom.2014.03.001

in tissues is affected by multipath effect, thus making receiver design a challenging issue. A desirable transmission scheme has to be designed to be multipath resilient, and in such a way as to facilitate the receiver decoding operations.

Limited resources. The low processing power and limited energy budget of nanorobots impose severe limitations in the design of a transmission scheme for opto-ultrasonic communications. Only very-low-complexity and low-power operations will be supported by future nanorobots. Therefore, both transmission and detection need to be characterized by limited signal processing complexity.

Health concerns. As discussed in Section 2, optical and acoustic energy imparted in tissues can cause undesired biological effects, e.g., heating and cavitation. Therefore, transmission schemes have to be designed in such a way as to avoid potential hazards for human health, and to avoid any irreversible damage of tissues.

Impulsive-only signals. As discussed in Section 3, optical energy radiation in tissues produces very-short temperature variations, hence very-short ultrasonic pulses. Based on this, it is clear that opto-ultrasonic communications must rely on an impulsive transmission scheme.

Interestingly enough, through very-short information-bearing carrierless ultrasonic pulses, one can jointly satisfy all the requirements discussed above. In fact, (i) the fine delay-resolution properties of very-short pulse transmissions can mitigate the multipath effect. When multipath replicas of pulses are received with a differential delay at least equal to the pulse width, they do not overlap in time with the original pulse. Moreover, (ii) the low duty cycle of pulsed transmissions reduces the impact of thermal and mechanical effects due to optical and acoustic energy absorption, which can be detrimental for human health. Furthermore, (iii) by tuning the transmission duty cycle one can find the right compromise between data rate and energy consumption based on the resources available to the nanorobots. Finally, (iv) carrierless impulsive transmissions, which do not require any frequency recovery technique, significantly simplify transceiver design, also lowering the nanorobots signal processing complexity and thus their energy consumption.

6.2. MAC layer

A MAC protocol for opto-ultrasonic communications has to be designed to jointly take into account the challenges posed by the ultrasonic intra-body channel, e.g., multipath and propagation delay among others, the limited capabilities of nanorobots, e.g., processing power and energy constraints, and the peculiarities of opto-ultrasonically generated signals, which are impulsive in nature and characterized by a very wide bandwidth. The desired solution is a low-complexity MAC protocol that allows users to fairly co-exist in the shared medium, and to maximize the network throughput while minimizing the protocol overhead, computational load and energy consumption.

MAC protocols designed for classical wireless sensor networks cannot directly be used for several reasons:

Frequency division. A frequency division approach requires each user to transmit a relatively narrowband signal in an allocated frequency band. First, narrowband signals are strongly affected by multipath effect, which can be significant in the ultrasonic intra-body communication channel, as discussed in Section 4. Second, the receiver design complexity increases due to the need for high-performing filters, modulators and demodulators required for frequency band selection. Besides, opto-ultrasonic generation produces ultra wideband and impulsive signals that do not easily meet the requirements of a frequency division scheme.

Time division. A time division approach may be inefficient due to the low propagation speed of sound in tissues, which would require long time guards to prevent collisions between adjacent time slots. However, in short-range communications, i.e., in the order of few hundreds of μm, the propagation delay is relatively low, as discussed in Section 4. Therefore, for highly localized clusters of nodes the inefficiencies introduced by long time guards can be negligible. Nevertheless, achieving local synchronization and slot allocation in a distributed, asynchronous, and possibly mobile environment can be challenging because of the limited resources and capabilities of nanorobots.

Carrier sensing. Carrier sensing techniques become inefficient when long propagation delays are considered. Besides, traditional carrier sensing is not meant to be used in carrierless systems such as an impulsive opto-ultrasonic system, because of the relatively low power spectral density. However, when propagation delays are acceptable, i.e., for short-range communications, alternative pulse-sense techniques can be leveraged to prevent collisions in the channel, and by introducing RTS/CTS mechanisms the hidden node problem can be mitigated. Clearly, using such contention-based techniques can potentially introduce latency and overhead, thus lowering the throughput and increasing the energy consumption.

Time hopping. Time-hopping has been designed specifically for impulse-based transmission schemes, e.g., Impulse Radio Ultra Wide Band (IR-UWB) [56]. By allowing transmissions that follow a pseudo-random time-schedule, this technique spreads pulses, or bursts of pulses, in time, in such a way as to provide a reasonable degree of robustness to collisions. However, generation and distribution of orthogonal time-hopping sequences can be challenging given the low processing power of nanorobots. Moreover, burst transmissions should be avoided to reduce potential undesirable bioeffects, as discussed in Section 2.

In [15], we presented Ultrasonic WideBand (UsWB), a low-complexity impulse-based PHY and MAC integrated protocol, where pulses are individually transmitted (i.e., not in bursts), following an adaptive time-hopping schedule with a superimposed pseudo-orthogonal spreading code. Similarly, in [57], the authors presented a low-complexity PHY-aware MAC solution, specifically designed for impulsive electromagnetic communications in the terahertz band, that considers single pulses spread in time, with no need of a pseudo-random time-hopping schedule.

6.3. Network layer

In a scenario of clustered nanonetworks deployed in several areas of the human body, the network layer will

Please cite this article in press as: G.E. Santagati, T. Melodia, Opto-ultrasonic communications for wireless intra-body nanonetworks, Nano Communication Networks (2014), http://dx.doi.org/10.1016/j.nancom.2014.03.001

be in charge of determining the optimal route to create a connection between these clusters of nanorobots, and/or to connect these with gateway devices, e.g., underskin microchips, that collect information and create a link between the intra-body nanonetworks and external macroscopic networks, i.e., the Internet. Again, important constraints in the design of networking protocols come from the characteristics of opto-ultrasonic intra-body communications among nanorobots. In fact, (i) propagation delays become significant, thus not negligible, when distances are in the range of centimeters, which can negatively affect the network operations; (ii) energy constraints due to health concerns and to the scarce nanorobots energy budget impose strict limitations in terms of protocol overhead; (iii) the limited processing power of nanorobots requires the design of low-complexity algorithms for implementing non-centralized routing protocols; finally, (iv) the heterogeneity of information, i.e., health status, reactive medication instructions, monitoring images and videos, may require special Quality of Service handling functionalities.

Given the challenges above, existing proactive and reactive routing protocols do not seem to be suitable for ultrasonic nanonetworks, because of their large protocol overhead and high latency in the establishment of path, which may be exacerbated by the low propagation speed of sound in tissues. On the other hand, multi-hop, multipath and position-based protocols, which use node position information to create multiple routes between source and destination, could represent a reliable and promising solution for intra-body networking. In fact, the geography of the body is fixed and well known, thus making localization easier than in classical extra-body networking environments. Moreover, by leveraging opto-ultrasonic impulsive transmissions, nodes can achieve accurate position estimation.

7. Conclusions

We discussed some fundamental aspects of nanoscale opto-ultrasonic communications in biological tissues and outlined the design challenges of opto-ultrasonic networking in the human body at different levels of the protocol stack. We first discussed the potential hazards posed by using opto-ultrasonic communications in the human body. Then, we modeled the generation, propagation and detection of opto-ultrasonic waves, and explored important tradeoffs such as the choice of an optimal transmission frequency and dependence of the bandwidth on the optical source size and duration. Finally, we discussed research challenges for the design of opto-ultrasonic nanonetworks of implantable devices at the physical (PHY), medium access control (MAC) and network layers of the protocol stack.

Acknowledgment

This work is based on material supported by the US National Science Foundation under grant CNS-1253309.

References

[1] G.E. Santagati, T. Melodia, Opto-ultrasonic communications in wireless body area nanonetworks, in: Proc. of IEEE Asilomar Conf. on Signals, Systems, and Computers, Pacific Grove, CA.
[2] I.F. Akyildiz, F. Brunetti, C. Blázquez, Nanonetworks: a new communication paradigm, Comput. Netw. 52 (2008) 2260–2279.
[3] J. Baker, A. Quintana, L. Piehler, M. Banazak-Holl, D. Tomalia, E. Raczka, The synthesis and testing of anti-cancer therapeutic nanodevices, Biomed. Microdev. 3 (2001) 61–69.
[4] W. Lu, M.P. Melancon, C. Xiong, Q. Huang, A. Elliott, S. Song, R. Zhang, L.G. Flores, J.G. Gelovani, L.V. Wang, G. Ku, R.J. Stafford, C. Li, Effects of photoacoustic imaging and photothermal ablation therapy mediated by targeted hollow gold nanospheres in an orthotopic mouse xenograft model of glioma, Cancer Res. 71 (2011) 6116–6121.
[5] I.F. Akyildiz, J.M. Jornet, Electromagnetic wireless nanosensor networks, Nano Commun. Netw. 1 (2010) 3–19.
[6] J.M. Jornet, J.C. Pujol, J.S. Pareta, Phlame: a physical layer aware MAC protocol for electromagnetic nanonetworks in the terahertz band, Nano Commun. Netw. 3 (2012) 74–81.
[7] M. Pierobon, I. Akyildiz, A physical end-to-end model for molecular communication in nanonetworks, IEEE J. Sel. Areas Commun. 28 (2010) 602–611.
[8] L. Parcerisa Giné, I.F. Akyildiz, Molecular communication options for long range nanonetworks, Comput. Netw. 53 (2009) 2753–2766.
[9] L. Galluccio, S. Palazzo, G.E. Santagati, Characterization of molecular communications among implantable biomedical neuro-inspired nanodevices, Nano Commun. Netw. 4 (2013) 53–64.
[10] I.F. Akyildiz, D. Pompili, T. Melodia, Underwater acoustic sensor networks: research challenges, Ad Hoc Netw. (Elsevier) 3 (2005) 257–279.
[11] T. Melodia, H. Kulhandjian, L. Kuo, E. Demirors, Advances in underwater acoustic networking, in: S. Basagni, M. Conti, S. Giordano, I. Stojmenovic (Eds.), Mobile Ad Hoc Networking: Cutting Edge Directions, second ed., John Wiley and Sons Inc., Hoboken, NJ, 2013, pp. 804–852.
[12] J.M. Reid, Medical Ultrasonics: Diagnostic Applications of Ultrasound, Proc. IRE 47 (1959).
[13] F.L. Thurstone, H.E. Melton, Biomedical ultrasonics, IEEE Trans. Ind. Electron. Control Instrum. 17 (1970).
[14] L. Galluccio, T. Melodia, S. Palazzo, G.E. Santagati, Challenges and implications of using ultrasonic communications in intra-body area networks in: Proc. of IEEE Intl. Conf. on Wireless On-demand Networked Systems, WONS, Courmayeur, Italy.
[15] G.E. Santagati, T. Melodia, L. Galluccio, S. Palazzo, Distributed MAC and rate adaptation for ultrasonically networked implantable sensors, in: Proc. of IEEE Conf. on Sensor, Mesh and Ad Hoc Communications and Networks (SECON) New Orleans, LA.
[16] G.E. Santagati, T. Melodia, Sonar inside your body: prototyping ultrasonic intra-body sensor networks, in: Proc. of IEEE Conference on Computer Communications (INFOCOM) Toronto, Canada.
[17] T. Hogg, R.A. Freitas, Acoustic communication for medical nanorobots, Nano Commun. Netw. (Elsevier) 3 (2012) 83–102.
[18] K. Shung, M. Zippuro, Ultrasonic transducers and arrays, IEEE Eng. Med. Biol. Mag. 15 (1996) 20–30.
[19] W. Kuhl, G. Schodder, F. Schroder, Condenser transmitters and microphones with solid dielectric for airborne ultrasonics, Acustica 4 (1954) 519.
[20] F. Akasheh, T. Myers, J.D. Fraser, S. Bose, A. Bandyopadhyay, Development of piezoelectric micromachined ultrasonic transducers, Sensors Actuators A 111 (2004) 275–287.
[21] B.T. Khuri-Yakub, Ömer Oralkan, Capacitive micromachined ultrasonic transducers for medical imaging and therapy, J. Micromech. Microeng. 21 (2011) 054004.
[22] R. Smith, A. Arca, X. Chen, L. Marques, M. Clark, J. Aylott, M. Somekh, Design and fabrication of nanoscale ultrasonic transducers, J. Phys. Conf. Ser. 353 (2012).
[23] M.W. Sigrist, F.K. Kneubuhl, Laser-generated stress waves in liquids, J. Acoust. Soc. Am. 64 (1978) 1652–1663.
[24] T. Buma, Y. Hou, S.-W. Huang, S. Ashkenazi, M. O'Donnell, High Frequency Optoacoustic Transducers for Ultrasonic and Photoacoustic Imaging, CRC Press, 2009, pp. 223–238. http://dx.doi.org/10.1201/9781420059922.ch18.
[25] A.G. Bell, Upon the production and reproduction of sound by light, J. Soc. Telegraph Eng. 9 (1880) 404–426.
[26] M. Xu, L.V. Wang, Photoacoustic imaging in biomedicine, Rev. Sci. Instrum. 77 (2006) 041101.
[27] J.Y. Suh, C.H. Kim, W. Zhou, M.D. Huntington, D.T. Co, M.R. Wasielewski, T.W. Odom, Plasmonic bowtie nanolaser arrays, Nano Lett. 12 (2012) 5769–5774.

[28] J.H. Lee, M. Khajavikhan, A. Simic, Q. Gu, O. Bondarenko, B. Slutsky, M.P. Nezhad, Y. Fainman, Electrically pumped sub-wavelength metallo-dielectric pedestal pillar lasers, Opt. Express 19 (2011) 21524–21531.
[29] Y.-J. Lu, J. Kim, H.-Y. Chen, C. Wu, N. Dabidian, C.E. Sanders, C.-Y. Wang, M.-Y. Lu, B.-H. Li, X. Qiu, W.-H. Chang, L.-J. Chen, G. Shvets, C.-K. Shih, S. Gwo, Plasmonic nanolaser using epitaxially grown silver film, Science 337 (2012) 450–453.
[30] P.A. Barnes, Studies of Laser Induced Breakdown Phenomena in Liquid Water, Ph.D. Thesis, Simon Fraser University (Canada), 1970.
[31] F. Loesel, M. Niemz, J. Bille, T. Juhasz, Laser-induced optical breakdown on hard and soft tissues and its dependence on the pulse duration: experiment and model, IEEE J. Quantum Electron. 32 (1996) 1717–1722.
[32] H.K. Park, D. Kim, C.P. Grigoropoulos, A.C. Tam, Pressure generation and measurement in the rapid vaporization of water on a pulsed-laser-heated surface, J. Appl. Phys. 80 (1996) 4072–4081.
[33] G. Paltauf, P.E. Dyer, Photomechanical processes and effects in ablation, Chem. Rev. 103 (2003) 487–518.
[34] A. Atalar, Photoacoustic effect as a liquid absorbance detector, Appl. Opt. 19 (1980) 3204–3210.
[35] A. N. S. Institute, L.I. of America, American National Standard for Safe Use of Lasers in Health Care Facilities: Standard Z136.1–2000, ANSI, Inc., New York 2000.
[36] K. Carnes, J. Drewniak, F. Dunn, In utero measurement of ultrasonically induced fetal mouse temperature increases, Ultrasound Med. Biol. 17 (1991) 373–382.
[37] J.L. Drewniak, K.I. Carnes, F. Dunn, In vitro ultrasonic heating of fetal bone, J. Acoust. Soc. Am. 86 (1989) 1254–1258.
[38] J.F. Lehmann, B.J. DeLateur, C.G. Warren, Heating produced by ultrasound in bone and soft tissue, Archives Phys. Med. Rehabil. 48 (1967) 397–401.
[39] S. Bushong, B. Archer, Diagnostic Ultrasound: Physics, Biology, and Instrumentation, Mosby, Incorporated, 1991.
[40] A. Doukas, T. Flotte, Physical characteristics and biological effects of laser-induced stress waves, Ultrasound Med. Biol. 22 (1996) 151–164.
[41] D.L. Miller, Safety assurance in obstetrical ultrasound, Sem. Ultrasound CT MRI 29 (2008) 156–164. Ultrasound in Obstetrics and Gynecology.
[42] B.T. Cox, S. Kara, S.R. Arridge, P.C. Beard, *k*-space propagation models for acoustically heterogeneous media: application to biomedical photoacoustics, Acoust. Soc. Am. 121 (2007).
[43] G.B. Arfken, H.J. Weber, F.E. Harris, Mathematical Methods for Physicists, Sixth Edition: A Comprehensive Guide, sixth ed., Academic Press, 2005.
[44] C.G.A. Hoelen, F.F.M. de Mul, A new theoretical approach to photoacoustic signal generation, J. Acoust. Soc. Am. 106 (1999) 695–706.
[45] M. O'Donnell, Y. Hou, J.-S. Kim, S. Ashkenazi, S.-W. Huang, L.J. Guo, Optoacoustic generation of high frequency sound for 3-d ultrasonic imaging in medicine, Eur. Phys. J. Spec. Top. 153 (2008) 53–58.
[46] A.A. Oraevsky, Gold and Silver Nanoparticles as Contrast Agents for Optoacoustic Tomography, CRC Press, 2009, pp. 223–238. http://dx.doi.org/10.1201/9781420059922.pt10.
[47] C.R. Hill, Ultrasonic Attenuation and Scattering by Tissues, John Wiley & Sons, Inc., 1978.
[48] F.P. Bolin, L.E. Preuss, R.C. Taylor, R.J. Ference, Refractive index of some mammalian tissues using a fiber optic cladding method, Appl. Opt. 28 (1989) 2297–2303.
[49] J. Hamilton, T. Buma, M. Spisar, M. O'Donnell, High frequency optoacoustic arrays using etalon detection, IEEE Trans. Ultrason. Ferroelectr. Freq. Control 47 (2000) 160–169.
[50] N. Hodgson, H. Weber, Optical Resonators: Fundamentals, Advanced Concepts, Applications, in: Springer Series in Optical Sciences, Springer, 2005.
[51] V.J. Sorger, R.F. Oulton, J. Yao, G. Bartal, X. Zhang, Plasmonic Fabry–Peŕot nanocavity, Nano Lett. 9 (2009) 3489–3493. PMID: 19673532.
[52] G. Hernandez, Fabry–Pérot Interferometers, in: African Studies Series, Cambridge University Press, 1986.
[53] V. Wilkens, Characterization of an optical multilayer hydrophone with constant frequency response in the range from 1 to 75 MHz, J. Acoust. Soc. Am. 113 (2003) 1431–1438.
[54] Y. Hou, S.-W. Huang, R. Witte, M. O'Donnell, S. Ashkenazi, Thin polymer etalon arrays for high-resolution photoacoustic imaging, J. Biomed. Opt. 13 (2008) 064033.
[55] P. Beard, F. Perennes, T. Mills, Transduction mechanisms of the Fabry–Perot polymer film sensing concept for wideband ultrasound detection, IEEE Trans. Ultrason. Ferroelectr. Freq. Control 46 (1999) 1575–1582.
[56] M.Z. Win, R.A. Scholtz, Ultra-wide bandwidth time-hopping spread-spectrum impulse radio for wireless multiple-access communications, IEEE Trans. Commun. 48 (2000).
[57] J. Pujol, J. Jornet, J. Pareta, Phlame: a physical layer aware mac protocol for electromagnetic nanonetworks, in: 2011 IEEE Conference on Computer Communications Workshops (INFOCOM WKSHPS), 2011, pp. 431–436.

G. Enrico Santagati is a Ph.D. student in the Department of Electrical Engineering at the University at Buffalo, The State University of New York (SUNY). He is currently working in the Wireless Networks and Embedded Systems Laboratory under the guidance of Professor Tommaso Melodia. He received his B.S. and M.S. in Telecommunication Engineering from the University of Catania (Italy) in 2010 and 2012, respectively. His current research interests are in ultrasonic intra-body networks and software defined radios.

Tommaso Melodia is an Associate Professor with the Department of Electrical Engineering at the University at Buffalo, The State University of New York (SUNY), where he directs the Wireless Networks and Embedded Systems Laboratory. He received his Ph.D. in Electrical and Computer Engineering from the Georgia Institute of Technology in 2007. He had previously received his "Laurea" and Doctorate degrees in Telecommunications Engineering from the University of Rome "La Sapienza", Rome, Italy, in 2001 and 2005, respectively. He serves in the Editorial Boards of IEEE Transactions on Wireless Communications, IEEE Transactions on Mobile Computing, and Computer Networks (Elsevier). He received a National Science Foundation CAREER award, and coauthored a paper that was recognized as the Fast Breaking Paper in the field of Computer Science by Thomson ISI Essential Science Indicators and a paper that received an Elsevier Top Cited Paper Award. His current research interests are in modeling, optimization, and experimental evaluation of wireless networks, with applications to cognitive and cooperative networking, ultrasonic intra-body networks, multimedia sensor networks, and underwater networks.

Please cite this article in press as: G.E. Santagati, T. Melodia, Opto-ultrasonic communications for wireless intra-body nanonetworks, Nano Communication Networks (2014), http://dx.doi.org/10.1016/j.nancom.2014.03.001